Western States Section of the Combustion Institute – Fall 2017 Meeting
Hosted by the University of Wyoming
October 2–3, 2017

Model sensitivities in LES predictions of buoyant methane fire plumes

Heeseok Koo[1,**], *John C. Hewson*[1], *Stefan P. Domino*[2], *and Robert C. Knaus*[2]

[1]*Fire Science and Technology, Sandia National Laboratories, PO Box 5800, MS 1135, Albuquerque, NM 87185-1135, USA* *
[2]*Compuational Thermodynamics and Fluid Mechanics, Sandia National Laboratories, PO Box 5800, MS 0828, Albuquerque, NM 87185-0828, USA*
**Corresponding author:* hkoo@sandia.gov

Abstract: A 1-m diameter methane fire plume has been studied using a large eddy simulation (LES) methodology. Eddy dissipation concept (EDC) and steady flamelet combustion models were used to describe interactions between buoyancy-induced turbulence and gas-phase combustion. Detailed comparisons with experimental data showed that the simulation is sensitive to the combustion model and mesh resolution. In particular, any excessive mixing results in a wider and more diffusive plume. As mesh resolution increases, the current simulations demonstrate a tendency toward excessive mixing.

***Keywords:* Fire plume, buoyant plume, LES, turbulent combustion, SIERRA Fuego**

1. Introduction

Fire plumes have been actively studied in recent years due to the associated impact and danger of industrial accidents involving leaking fuel [1–3]. A number of experiments have been performed to understand the physics [4–8] from which empirical models were obtained [9–11]. Simulating fire plumes, however, has several modeling challenges such as flame ignition/extinction, turbulence-combustion-radiation interaction, laminar-turbulence transition, soot formation, and the fact that they are dominated by a relatively slow, buoyancy-driven flow. Combusting plumes have been a target for many fire modelers [3, 12–16] and efforts by several researchers were compared and discussed on the 2017 Measurement and Computation of Fire Phenomena (MaCFP) workshop, which offered a central forum for fire model validation [17].

LES is becoming the state-of-the-art tool for modeling turbulent combustion and is also widely used for fire calculations [17], though the level of resolution varies and also places simulations in a regime where most of the turbulent kinetic energy is modeled. The EDC approach with fast chemistry and the steady flamelet models are frequently used turbulent combustion models in the fire community [18–20]. These models were used in this study, including assumptions that local extinction/ignition and flame liftoff are not critical in predicting pool fires.

FLAME (the Fire Laboratory for Accreditation of Models by Experimentation) is the high-fidelity, large-scale, controlled, indoor facility for fire validation experiments that is constructed

*Sandia National Laboratories is a multimission laboratory managed and operated by National Technology and Engineering Solutions of Sandia, LLC., a wholly owned subsidiary of Honeywell International, Inc., for the U.S. Department of Energy's National Nuclear Security Administration under contract DE-NA0003525.

and maintained by Sandia National Laboratories for pool fire and related experimental studies [2]. A number of data sets are available from experiments performed using different gaseous or liquid fuels, varying pool sizes, under changing operating conditions for various types of fires [4, 5, 21–23]. Across two different versions of the facility, FLAME allows laser diagnostics such as PIV and PLIF at scales larger than typically possible [4] along with heat flux gauges [23], and more recently, coherent anti-Stokes Raman scattering (CARS) [22]. The methane pool fire case that current study focuses on were performed in an older version of the facility from which mean and rms velocities are available [4].

The focus of this paper is to understand sensitivity of the plume predictions to various modeling and mesh choices. In particular, the effects of domain shape, mesh resolution, combustion models and boundary conditions were verified. SIERRA/Fuego [20], an in-house low-Mach turbulent combustion code developed by Sandia National Laboratories, was used for the simulations. The next two sections describe target problem and numerical models, before providing simulation results from Sec. 4.

2. Experimental Configuration

Figure 1 shows an outer view of the facility as well a diagram of the aforementioned FLAME facility. The internal test section of the facility has a 5.8m×5.8m square area with a converging hood 4.5 m above the fuel inlet. A 1m-diameter fuel inlet is located at the middle of the 2m-diameter pedestal-like structure that simulates a ground plane. Air is injected at an outer-ring which lies at 3m below the fuel-inlet height. A cylindrical radiation shield, colored in orange in Fig. 1 in the middle, is installed from the bottom up to 0.9m above the fuel-inlet height to minimize any asymmetric behavior.

PIV measurements were performed on the center plane on a 1m×1m area right above the fuel inlet. Table 1 summarizes three experimental conditions published and available. Here, test #24 is simulated which is in the middle in terms of its fuel-air flow rate ratio.

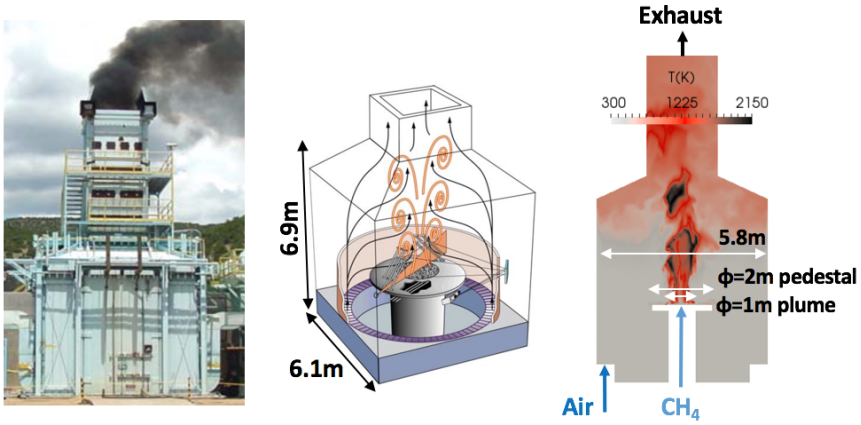

Figure 1: Picture and figures of the FLAME experimental facility

Test No.	Fuel inlet velocity (m/s)	Heat release rate (MW)	Inlet air velocity (m/s)	Equivalence ratio (global)
14	0.074	1.59	0.323	0.19
24	0.097	2.07	0.327	0.25
17	0.117	2.61	0.299	0.34

Table 1: Available test cases

3. Model Details

Simulations are conducted using an unstructured control-volume finite-element code [20, 24, 25], a component of Sandia National Laboratories SIERRA thermal-fluids code suite. The package has a capability of integrating different physics in multiple phases. SIERRA/Fuego, used for the current study, is a low-Mach flow solver suited for non-reacting and reacting flows. Various RANS (Reynolds-averaged Navier-Stokes) and LES turbulence models are available in the code. For LES, constant-coefficient and dynamic versions of the Smagorinsky model and subgrid-scale kinetic energy one-equation models are available. In this study, both Smagorinsky and one-equation models are used to describe the subfilter process with pre-defined coefficients.

Two approaches are used for the gas-phase combustion. In the first approach, the gas-phase combustion is closed with the eddy-dissipation concept (EDC) with fast chemistry [26]. An arbitrary hydrocarbon fuel is decomposed into CO and H_2 at the first step, while the intermediate species, CO and H_2, are further oxidized in the second step provided oxygen is still sufficient. This approach models CO, and potentially soot, in the fuel-rich case. Enthalpy and species mass fraction equations are Favre-filtered along with momentum. Radiative heat transfer is incorporated by solving a radiation transport equation.

In the second approach, the gas-phase combustion is described using a steady flamelet model where a set of one-dimensional flamelets are tabulated for look-up in the computation [27]. The transport equation for a conserved scalar, namely fuel-oxidizer mixture fraction, is solved along with momentum equations. Mixture fraction replaces many variables in EDC, such as enthalpy, species mass fraction, and even radiation, which allows a cost effective computation. A mechanism that contains detailed methane reaction (GRI-Mech 2.11 [28]) and the Flamemaster program [29] were used in the tabulation. A subfilter closure using an assumed, clipped Gaussian PDF was used, with the variance of the mixture fraction being estimated using a gradient model. Tabulated file size was reduced using an adaptive coarsening technique.

4. Domain Sensitivity

The effect of the computational domain shape is discussed in this section. Two configurations were used to assess the effect, marked as ‘Full geometry’ and ‘Cylindrical’. The first mesh includes as many details of the facility as possible (Fig. 2, left). Air and fuel inlets are colored by blue and red in the figure. The oxidizer stream is expected to exhibit recirculation in the unoccupied space below fuel injection pedestal. Moreover, flame interaction with downstream constriction imposed by the upper hood and exhaust chamber is fully considered in this configuration. For meshing convenience, the cylindrical radiation shield is assumed to extend to the top. All elements are hexahedra, except for a small region around the hood where tetrahedral and pyramid elements are

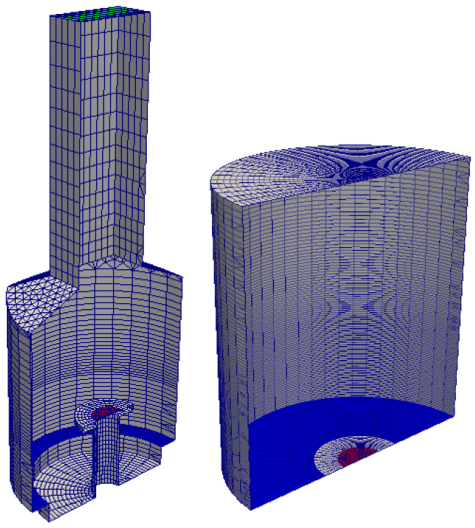

Figure 2: Cut views of full geometry (left) and simplified cylindrical (right) computational domain. Surfaces are colored by fuel inlet (red), air inlet (blue), and wall (grey).

used. A uniform bulk velocity is assumed at both fuel and air inlets; there are no perturbations used to represent inflowing air fluctuations. Mesh and boundary condition information is listed in Table 2. An adiabatic condition is used for all wall surfaces.

A simplified cylindrical domain is also tested (Fig. 2, right) that preserves the same facility diameter of 5.8m and similar height (5m rather than 4.5m). Uniform air velocity is assumed at the coflow section so that total oxidizer flow rate is preserved with the full geometry simulation; this limits the existance of . The top exit boundary, however, is confined to the center part with a diameter of 2m to avoid asymmetric plume development. All elements are hexahedra. Different resolutions are tested using the cylindrical domain. Table 2 lists the meshes used in this study. Around the base of the plume is a nearly uniform mesh with the characteristic cell size listed in the table. Away from the base of the plume, the mesh is progressively coarsened.

Domain shape	Total elements	Mesh size near plume	Air velocity	Fuel velocity
Full geometry	1.7M	2.5cm	0.33	0.097
Cylindrical	0.23M	4cm	0.14	0.097
Cylindrical	1.6M	2cm	0.14	0.097
Cylindrical	7.0M	1cm	0.14	0.097

Table 2: List of the simulated meshes

Figure 3 compares mean velocity profiles of the two domains at three different heights, 0.3m, 0.5m, and 0.9m, from the fuel inlet location. The coarsest results are compared here using the flamelet model—the 1.7M and 0.23M meshes. Peak predicted velocities at the core are comparable to experimental velocities suggesting some general prediction of the buoyant forcing. The full geometry prediction appears to show larger velocities in the tail with larger radial entrainment velocities, indicating stronger external turbulent fluctuations and entrainment or a broader buoyant forcing.

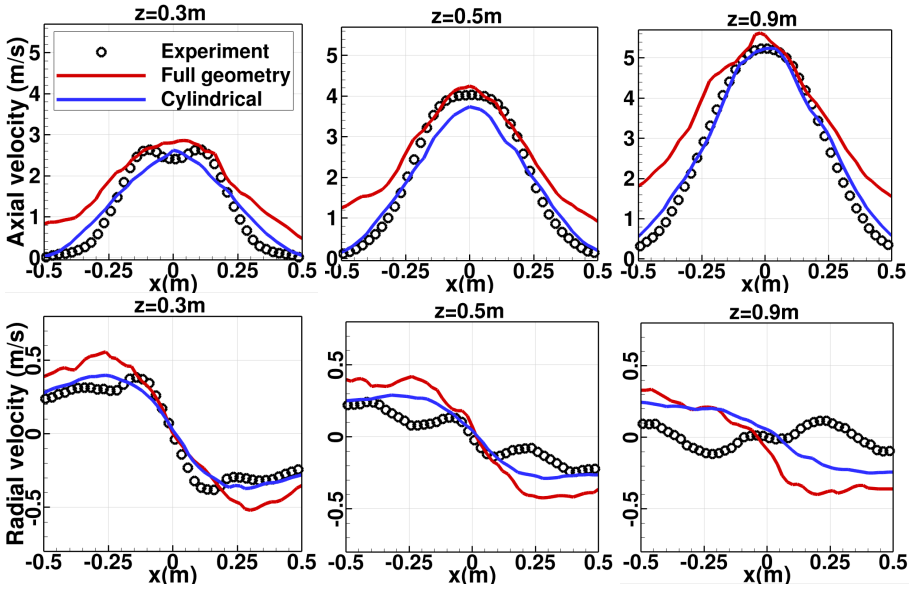

Figure 3: Effect of the configuration geometry for predictions compared to the experimental data [4]. Averaged axial (top) and radial (bottom) velocities at different distances from the fuel inlet.

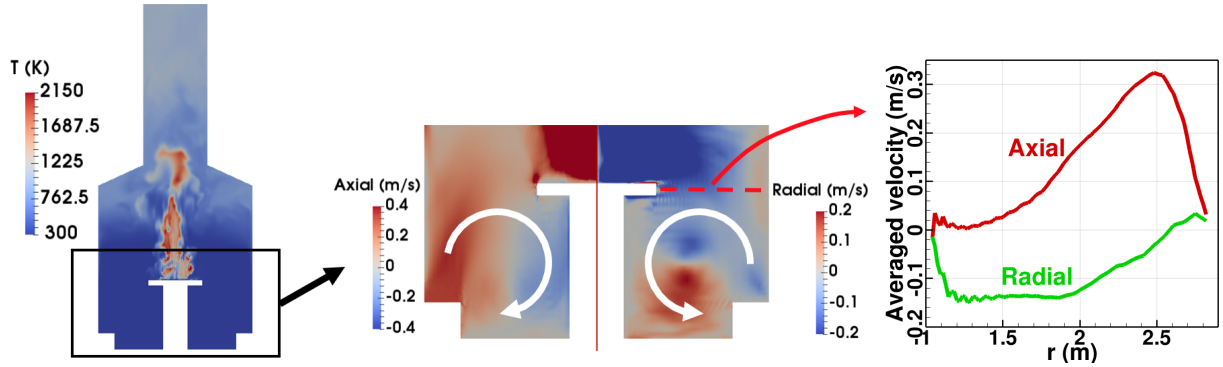

Figure 4: A temperature snapshot (left) and averaged axial and radial velocity contours (middle). On the right is averaged velocity profiles along the red dashed line.

The full geometry simulation is expected to offer a better description of the coflowing oxidizer stream at the fuel injection level. Figures 4 provide a snapshot and averaged velocity contours below the plume source at the middle plane. Also provided is the averaged axial and radial velocity profiles at the fuel plume height. Recirculation develops below the pool (white circlular arrows in Fig. 4) in this simulation, and this weakens the vertical flow, tending to convert it to a radial inflow just below the fuel source. This large scale motion appear to contribute to the diffuse plume profile in this simulation (Fig. 3). We note that the outer region is only coarsely resolved, and further assessment of the upstream coflow effect is possible. Meanwhile, it was found that the convergence associated with the top hood affects on the statistics only minimally for this simulation.

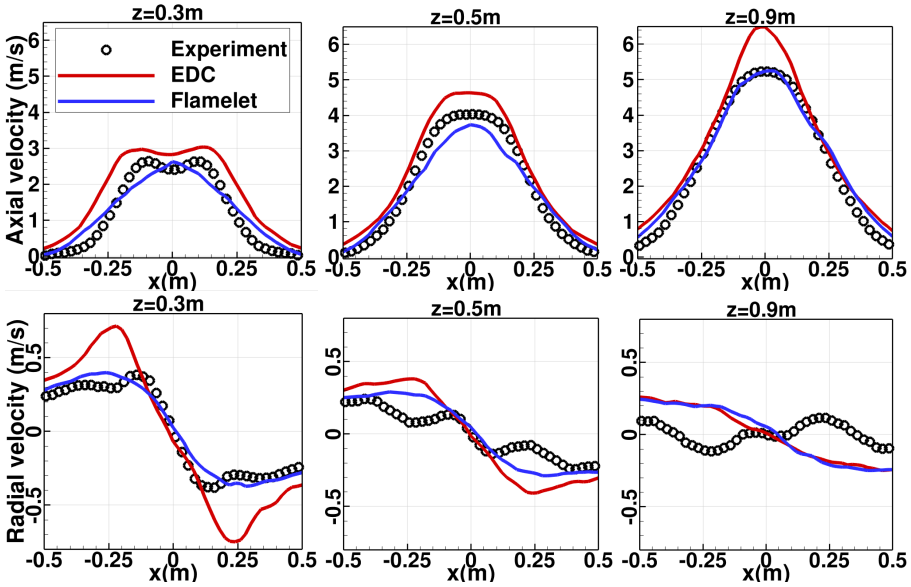

Figure 5: Effect of combustion model compared to the experimental data, for axial (top) and radial (bottom) velocities.

5. Combustion Model Sensitivity

Using the cylindrical domain, two combustion models—the EDC and flamelet models—were tested at three different mesh resolutions. In Fig. 5, the two models were compared on the coarsest 0.23M mesh. The EDC results in a higher centerline velocity which suggests that the reaction rate is over-predicted at this resolution leading to greater buoyant forcing. The plume width is overall similar regardless of the model choice. At the same time, the EDC model successfully captures two peaks and a local minima in the core velocity profile at 0.3 m location, which is missed with flamelet approach at this resolution.

Figure 6 compares averaged temperature contours near the plume for different models and resolutions. The EDC prediction suggests more intense fuel-air mixing in the near-field than the flamelet prediction. This EDC prediction suggests a continuous reaction zone from the plume edge as seen in the experimental pictures [4]. The continuous high-temperature bands are associated with the two peaks in the velocity profile (Fig. 5). Meanwhile, high scalar variance near the plume exit leads to a lower prediction of the mean flame temperature for this coarse mesh. Simulations using better grid resolution better resolve the near-fuel-source temperature field as shown in the same figure; this will be further discussed in the following section.

6. Mesh Resolution Sensitivity

The two combustion models were tested on different meshes with varying levels of resolution. Resolution was varied by doubling the resolution in the near plume region, but the mesh stretching was more aggressive for these cases to manage the overall simulation cost so that the actual mesh size does not increase as the near-plume resolution cubed. The flamelet model is applied at all three resolutions, 0.23M, 1.6M, and 7.0M meshes, and EDC is tested on the 0.23M and 1.6M meshes.

Figure 7 compares mean velocity profiles for different resolutions when the flamelet model

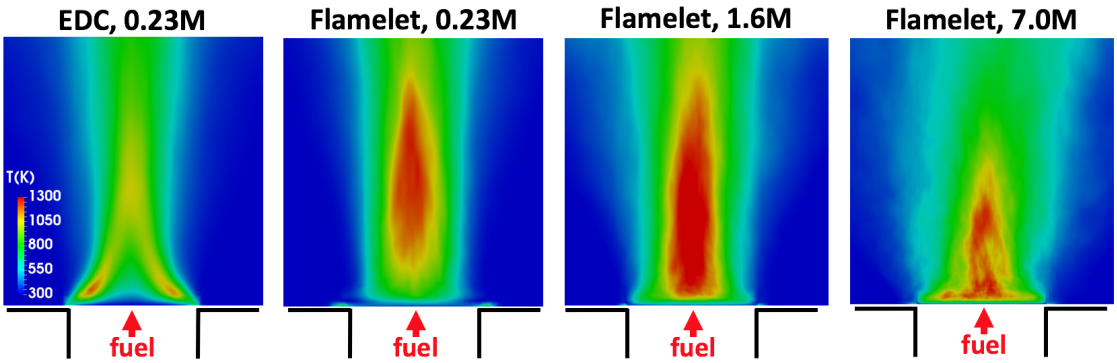

Figure 6: Averaged temperature contours. Note that statistics of 7.0M mesh case are not yet statistically converged.

was used. It shows that the coarser resolution better predicts flow statistics for these cases. As the mesh resolution increases, the plume appears to become weaker and wider. This is associated with stronger lateral entrainment. Figure 6 and 8 show averaged temperature and velocity fields for the three resolutions. The size of the high temperature area in Fig. 6 indicates that the middle resolution (1.6M) results in a broader high temperature region than the other cases. However, a more prominent tendency is an increased resolution of high temperatures nearer the pool surface. This is likely indicative of greater fual-oxidizer mixing right above the fuel exit plane, which is linked to the larger radial entrainment velocity (Fig. 8). This larger radial velocity increases turbulent intensity by inducing lateral motion of the plume, which diffuses the plume (lower velocity peak at Fig. 7). The enhanced plume motion increases mixing efficiency, and in turn, brings the high temperature regions even closer to the plume surface. EDC, with the higher resolution mesh, also predicts higher temperature regions nearer the plume compared to the lower resolution (not shown here). While statistics are not ready yet, this tendency with respect to the mesh resolution is expected to follow that of the flamelet model.

Figure 9 shows that plume puffing occurs at a 1Hz frequency when the 7.0M mesh and flamelet model is used. The motion is slower than the experiment of 1.5Hz. This repeated motion might be affected by the strong crossflow, and the relation between the puffing frequency and entrainment fluctuations is currently under investigation.

Three causes can be imagined regarding predictions of apparently stronger mixing and entrainment with increased mesh refinement than observed in the experiment. First, buoyancy-driven mixing may be incorrectly predicted, and this might influence the statistics. Second, laminar-turbulence transition is often difficult to predict with LES, and this might alter mixing levels. The plume injection is in low velocity ($\sim$0.1m/s) and low Reynolds number ($\sim$6000). For these results, there are no stochastic perturbations introduced into the inflow to represent fluctuations. With the size of the device, it is unlikely that the fuel inlet is spatially uniform with a constant mass flux at all locations throughout the duration of the test. In other simulations not presented here, inlet fluctuations can have a strong effect. Third, the stretched mesh moving away from the fuel inlet may significantly affect the predictions; this stretching is most severe at the highest resolutions.

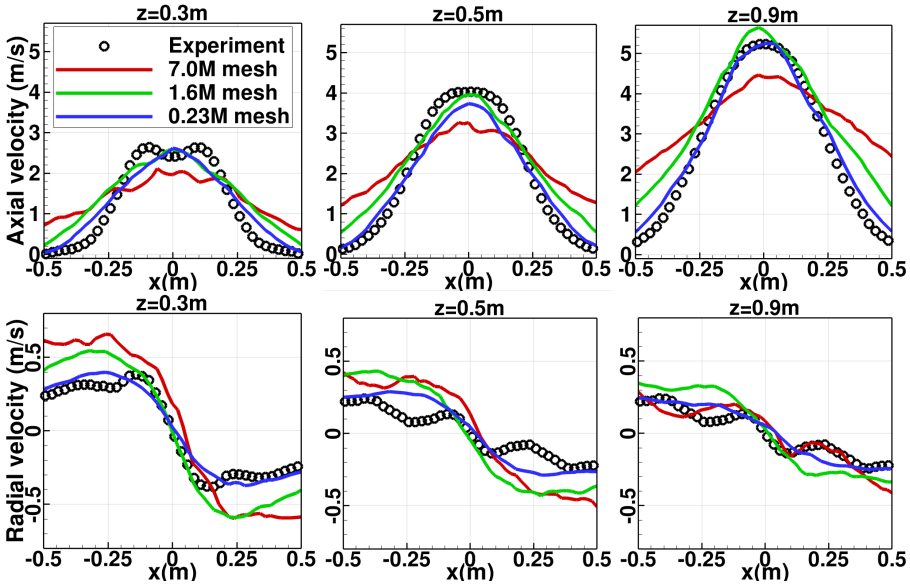

Figure 7: Effect of mesh resolution compared to the experimental data, for axial (top) and radial (bottom) velocities.

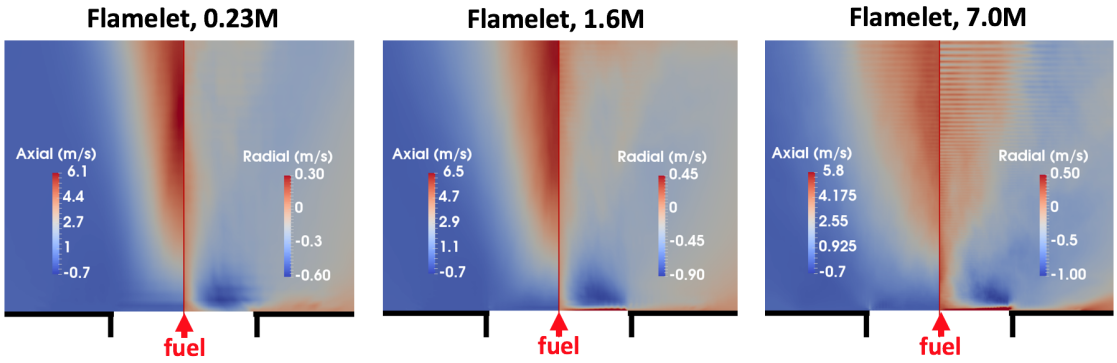

Figure 8: Averaged axial and radial velocity contours of three resolutions.

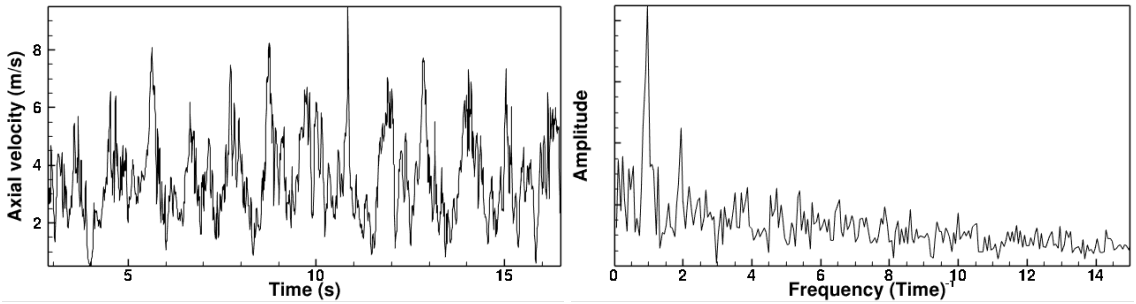

Figure 9: Axial velocity profile in time (left) and in frequency domain (right) at centerline, 0.5m height, from 7.0M flamelet simulation.

7. Conclusion

A series of LES predictions of a 1-m diameter methane fire plume scenario are preformed to understand the effect of mesh resolution and geometric fidelity have on the predictions. First, the full geometry associated with structure containing the experimental facility is compared with a simplified cylindrical configuration. While the full geometry might predict more a realistic coflow velocity profile at the fuel inlet height, the velocity statistics were not improved compared to that of the simplified geometry simulation. Secondly, the combustion model comparison showed that the flamelet approach better matches the velocity statistics while EDC model simulations predict temperature contours that are intuitively appealing with more apparent flame attachment at the fuel inlet edges. Lastly, the models were tested at various mesh resolutions. At the moment, the higher resolution meshes result in excessive mixing and therefore, a diffused plume. However, the coarsest mesh flamelet model prediction, which actually shows the best results among the simulations, shows evidence that the mixture fraction variance is too large, leading to lower averaged flame temperatures near the fuel inlet. At this stage it is not possible to evaluate whether the coarse mesh 'predictivity' is coincidental or not, and further assessment of uncertainties will continue to bring clarification to these results.

Acknowledgement

Sandia National Laboratories is a multimission laboratory managed and operated by National Technology and Engineering Solutions of Sandia, LLC., a wholly owned subsidiary of Honeywell International, Inc., for the U.S. Department of Energy's National Nuclear Security Administration under contract DE-NA0003525. This work was supported by Sandia National Laboratories' Advanced Simulation and Computing program through the Physics and Engineering Models subprogram and the Verification and Validation subprogram elements.

References

[1] T. K. Blanchat, V. F. Nicolette, W. D. Sundberg, and V. G. Figueroa, Well-Characterized Open Pool Experiment Data and Analysis for Model Validation and Development, SAND 2006-7508 (2006).

[2] T. K. Blanchat, Characterization of the Air Source and the Plume Source at FLAME, SAND 2001-2227 (2001).

[3] G. Maragkos and B. Merci, Large Eddy Simulations of CH4 Fire Plumes, Flow Turbulence and Combustion 99 (2017) 239–278.

[4] S. Tieszen, T. O'Hern, R. Schefer, E. Weckman, and R. Schefer, Experimental study of the effect of fuel mass flux on a 1-m-diameter methane fire and comparison with a hydrogen fire, Combustion and Flame 139 (2004) 126–141.

[5] T. K. Blanchat and J. Suo-Anttila, Hydrocarbon Characterization Experiments in Fully Turbulent Fires - Results and Data Analysis, SAND 2010-6377 (2010).

[6] B. J. McCaffrey, PurelyBuoyantDiffusionFlames:Someexperimentalresults, National Bureau of Standards, NBSIR 79-1910, 1979.

[7] B. M. Cetegen, E. E. Zukoski, and T. Kubota, Entrainment and Flame Geometry of Fire Plumes, National Bureau of Standards, NBS-GCR 80-402, 1980.

[8] E. J. Weckman and A. B. Strong, Experimental investigation of the turbulence structure of medium-scale methanol pool fires, Combustion and Flame 105 (1996) 245–266.

[9] H. Koseki, Large Scale Pool Fires: Results of Recent Experiments, Fire Safety Science 6 (2000) 115–132.

[10] L. Hu, A review of physics and correlations of pool fire behavior in wind and future challenges, Fire Safety Journal 91 (2017) 41–55.

[11] A. Hamins, J. C. Yang, and T. Kashiwagi, An experimental investigation of the pulsation frequency of flames, Symposium (International) on Combustion 24 (1992) 1695–1702.

[12] A. Luketa, Assessment of Simulation Predictions of Hydrocarbon Pool Fire Tests, SAND 2010-2511 (2010).

[13] A. L. Brown, K. J. Dowding, V. F. Nicolette, and T. K. Blanchat, Fire Model Validation for Gas Temperatures and Radiative/Convective Partitioned Heat Flux, Fire Safety Science 9 (2008) 93–104.

[14] A. R. Black, Numerical Predictions and Experiment Results for a 1m Diameter Methane Fire, ASME 2005 International Mechanical Engineering Congress and Exposition (2005).

[15] A. Trouve, CFD Modeling of Large-Scale Pool Fire, The Second International Energy 2030 Conference (2008).

[16] W. M. Eldredge, J. N. Thornock, and P. J. Smith, Development, Verification, and Validation of the Responsive Boundary Model for Pool Fire Simulations, 20th AIAA Computational Fluid Dynamics Conference (2011).

[17] *The 1st Measurement and Computation of Fire Phenomena (MaCFP) Workshop*, 2017, URL: `http://www.iafss.org/macfp/`.

[18] K. McGrattan, S. Hostikka, R. McDermott, J. Floyd, C. Weinschenk, and K. Overholt, Fire Dynamics Simulator Technical Reference Guide Volume 1: Mathematical model, NIST Special Publication 1018 Sixth Edition (2014).

[19] Z. Chen, J. Wen, B. Xu, and S. Dembele, Large Eddy Simulation of Fire Dynamics with the Improved Eddy Dissipation Concept, Fire Safety Science 10 (2011) 795–808.

[20] *SIERRA Low Mach Module: Fuego User Manual – Version 4.42, SAND2016-10164*, Sandia National Laboratories, 2016.

[21] P. DesJardin, T. O'Hern, and S. Tieszen, Large eddy simulation and experimental measurements of the near-field of a large turbulent helium plume, Physics of Fluids 16 (2004) 1866–1883.

[22] K. Frederickson, S. P. Kearney, A. Luketa, J. C. Hewson, and T. W. Grasser, Dual-Pump CARS Measurements of Temperature and Oxygen in a Turbulent Methanol-Fueled Pool Fire, Combustion Science and Technology 182 (2010) 941–959.

[23] T. Blanchat, T. O'Hern, S. Kearney, A. Ricks, and D. Jernigan, Validation experiments to determine radiation partitioning of heat flux to an object in a fully turbulent fire, Proceedings of the Combustion Institute 32 (2009) 2511–2518.

[24] S. R. Tieszen, S. P. Domino, and A. R. Black, Validation of a Simple Turbulence Model Suitable for Closure of Temporally-Filtered Navier-Stokes Equations Using a Helium Plume, Sandia National Laboratories, Albuquerque, NM, USA, (2005).

[25] A. Luketa, V. Romero, S. Domino, D. Glaze, M. Sherman, and V. Figueroa, Validation and uncertainty quantification of Fuego simulations of calorimeter heating in a wind-driven hydrocarbon pool fire, Sandia National Laboratories, Albuquerque, NM, USA, (2009).

[26] B. F. Magnussen, On the Structure of Turbulence and a Generalised Eddy Dissipation Concept for Chemical Reactions in Turbulent Flow, 9th AIAA Aerospace Science Meeting (1981).

[27] N. Peters, Turbulent Combustion, Cambridge University Press, 2000.

[28] C. Bowman, R. Hanson, D. Davidson, J. W.C. Gardiner, V. Lissianski, G. Smith, D. Golden, M. Frenklach, and M. Goldenberg, URL: `http://www.me.berkeley.edu/gri_mech/`.

[29] H. Pitsch, URL: `https://www.itv.rwth-aachen.de/index.php?id=flamemaster`.